THE JOURNAL OF BIOLOGICAL CHEMISTRY VOL. 289, NO. 35, pp. 24275–24288, August 29, 2014

The Mammalian Ste20-like Kinase 2 (Mst2) Modulates Stress-induced Cardiac Hypertrophy*

Received for publication, March 3, 2014, and in revised form, July 16, 2014 Published, JBC Papers in Press, July 17, 2014, DOI 10.1074/jbc.M114.562405

Min Zi[‡1], Arfa Maqsood[‡1], Sukhpal Prehar[‡1], Tamer M. A. Mohamed[‡], Riham Abou-Leisa[‡], Abigail Robertson[‡], Elizabeth J. Cartwright[‡], Simon G. Ray[§], Sangphil Oh[¶], Dae-Sik Lim[¶], Ludwig Neyses[‡], and Delvac Oceandy[‡2]

From the [‡]Institute of Cardiovascular Sciences, University of Manchester and Manchester Academic Health Science Centre, Manchester M13 9PT, United Kingdom, the [§]Department of Cardiology, South Manchester University Hospital and Manchester Academic Health Science Centre, Manchester M23 9LT, United Kingdom, and the [¶]Department of Biological Sciences, National Creative Research Initiatives Center, Graduate School of Nanoscience and Technology (WCU), Korea Advanced Institute of Science and Technology, Daejeon 305-701, Korea

Background: The role of components of the Hippo signaling pathway in mediating pathological cardiac hypertrophy is incompletely understood.
Results: Genetic ablation of *Mst2* reduces pathological cardiac hypertrophic response in adult mice.
Conclusion: Mst2 regulates stress-induced cardiac hypertrophy by modulating the Raf1-ERK1/2 pathway.
Significance: Mst2 might become a novel therapeutic target to reduce pathological hypertrophy.

The Hippo signaling pathway has recently moved to center stage in cardiac research because of its key role in cardiomyocyte proliferation and regeneration of the embryonic and newborn heart. However, its role in the adult heart is incompletely understood. We investigate here the role of mammalian Ste20-like kinase 2 (Mst2), one of the central regulators of this pathway. *Mst2*$^{-/-}$ mice showed no alteration in cardiomyocyte proliferation. However, *Mst2*$^{-/-}$ mice exhibited a significant reduction of hypertrophy and fibrosis in response to pressure overload. Consistently, overexpression of *MST2* in neonatal rat cardiomyocytes significantly enhanced phenylephrine-induced cellular hypertrophy. Mechanistically, Mst2 positively modulated the prohypertrophic Raf1-ERK1/2 pathway. However, activation of the downstream effectors of the Hippo pathway (Yes-associated protein) was not affected by Mst2 ablation. An initial genetic study in mitral valve prolapse patients revealed an association between a polymorphism in the human *MST2* gene and adverse cardiac remodeling. These results reveal a novel role of Mst2 in stress-dependent cardiac hypertrophy and remodeling in the adult mouse and likely human heart.

Cardiac hypertrophy is a key pathological process in the development of heart failure (1). It is believed that in the adult heart, enlargement of cardiomyocytes is the major mechanism involved in hypertrophy (2) rather than cellular proliferation. However, recent studies have suggested that in both human and mouse, cardiomyocytes have the capacity to regenerate (3, 4). Thus, characterization of molecules that are involved in regulating cellular proliferation in the context of cardiac hypertrophy is an important focus of study.

The emerging Hippo signaling pathway has been regarded as the key regulator of cell proliferation and organ size control. Ablation of *Drosophila hippo* results in increased proliferation, resistance to apoptosis, and organ enlargement (5). The mammalian orthologs of *hippo* are mammalian ste-20-like kinase 1 (Mst1)[3] and Mst2. Conditional ablation of both *Mst1* and *Mst2* in mouse hepatocytes (6) and intestinal epithelium (7) resulted in massive cellular proliferation, increased organ size, and development of multifocal carcinoma. In both models, reduction in Yes-associated protein (YAP) phosphorylation (the mammalian ortholog of *yorkie*), and consequently its nuclear translocation, appeared to be the responsible mechanism.

The Hippo pathway is also involved in regulating cardiomyocyte proliferation during embryonic development and in neonates. Ablation of *Salvador* in mouse cardiomyocytes, which effectively reduced both Mst1 and Mst2 function, resulted in enhanced cardiomyocyte proliferation during embryonic development and in newborn mice (8). Moreover, overexpression of constitutively active YAP in the heart resulted in enhanced cardiomyocyte proliferation in embryonic and newborn mice, whereas YAP ablation caused a significant reduction of cardiomyocyte number, leading to embryonic lethality (9, 10). However, the precise role of the mammalian *Hippo* orthologs in the adult heart is not clear. Recent studies have described Mst1 as a regulator of apoptosis (11, 12) and autophagy (13) in the heart. However, the role of Mst2 in adult heart is not known. Here, we found a novel role for Mst2 in stress-dependent cardiac hypertrophy and remodeling via

* This work was supported by British Heart Foundation Intermediate Fellowship Grant FS/09/046/28043 and British Heart Foundation Project Grants PG/11/23/28801 and PG/13/12/30017 (to D. O.).
[1] These authors contributed equally to this work.
[2] A recipient of a British Heart Foundation Intermediate Basic Science Research Fellowship. To whom correspondence should be addressed: Institute of Cardiovascular Sciences, University of Manchester and Manchester Academic Health Science Centre, 5.002 AV Hill Bldg., Oxford Rd., Manchester M13 9PT, UK. Tel.: 44-161-275-1772; E-mail: delvac.oceandy@manchester.ac.uk.

[3] The abbreviations used are: Mst1, mammalian Ste-20-like kinase 1; ERK, extracellular signal regulated kinase; YAP, Yes-associated protein; TAC, Transverse aortic constriction; NRCM, neonatal rat cardiomyocyte(s); BNP, brain natriuretic peptide; pHH3, phospho-histone H3; HW/BW, heart weight/body weight ratio; LV, Left ventricular; SNP, single nucleotide polymorphism.

modulation of the prohypertrophic Raf1-ERK1/2 pathway in the adult mouse heart and likely in human heart.

EXPERIMENTAL PROCEDURES

Animal Model—Mice with targeted deletion of the *Mst2* gene were used in this study (14). We used 8–10-week-old male *Mst2*$^{-/-}$ mice for pressure overload induced hypertrophy experiments. Mice were maintained on 129Sv/J × C57Bl/6 genetic background. Age- and sex-matched wild type littermates were used as controls. Animal studies were performed in accordance with the United Kingdom Animals (Scientific Procedures) Act 1986 and were approved by the University of Manchester Ethics Committee.

Human Heart Tissues—Heart extracts from human heart failure and normal subjects were obtained from Asterand, who obtained informed consent for the use of human tissue samples and approval by the United Kingdom Human Tissue Authority.

In Vivo Hypertrophy Model—Mice were subjected to transverse aortic constriction (TAC) to generate pressure overload-induced hypertrophy model as described previously (15). TAC was conducted using a 7-0 silk suture that was tied to a 27-gauge constriction at the aortic arch, which will produce ~25–30 mmHg pressure gradient between the left and right carotid artery.

Echocardiography and Hemodynamic Analyses in Mice—Mouse echocardiography was conducted using an Acuson Sequoia C256 system (Siemens) following a protocol described previously (16). For hemodynamic analysis, we used a 1.4F pressure-volume catheter (SPR-839) and a pressure volume system (Millar Instruments). Cardiac function was assessed using a protocol described previously (16).

Plasmid Constructs and Adenoviruses—Plasmids containing either human wild type Mst2 or mutant Mst2 K56R were a gift of Dr. Jonathan Chernoff (17) (Addgene plasmid nos. 12205 and 12206). Adenoviruses were generated using Gateway vector system (Invitrogen). To generate Mst2 deletion mutants we amplified Mst2-ΔC (containing amino acids residue 1–277) by PCR. Fragment was then cloned to pENTR-11 (Invitrogen) to allow generation of adenoviruses by the Gateway system.

Neonatal Rat Cardiomyocyte Isolation—Neonatal rat cardiomyocytes (NRCM) and cardiofibroblasts were isolated from 1–3 day old Sprague-Dawley rat neonates using an established protocol (18). Cells obtained from the digestion of rat neonate hearts were plated in medium containing 68% DMEM, 17% medium 199, 10% horse serum, and 5% fetal bovine serum and incubated for 60 min at 37 °C to allow attachment of cardiac fibroblasts. Then, supernatants containing cardiomyocytes were plated on Primaria plates (BD Biosciences) using similar plating medium containing 1 μM BrdU. Neonatal rat cardiofibroblasts were used for experiments after at least three passages of culture in medium containing 10% FBS.

Adult Cardiac Fibroblast Isolation—Adult cardiac fibroblasts were isolated from *Mst2*$^{-/-}$ and WT mice. Heart tissues were digested with 1.5 mg/ml collagenase A (Roche Applied Science) and 0.15 mg/ml protease (Sigma). Cells were cultured in DMEM containing 20% FBS prior to experiments.

Cellular Hypertrophy Experiment—For cardiomyocyte hypertrophy experiments, NRCM were infected with the indicated adenovirus for 24 h and then treated with 20 μM phenylephrine for 48 h with or without the addition of ERK1/2 inhibitor FR180204 (Millipore) at a final concentration of 50 μM. NRCM were stained with anti-α-actinin antibody (Sigma) and the cell size was then measured using ImageJ software. Brain natriuretic peptide (BNP) promoter activation was analyzed using a BNP-luciferase adenoviral reporter construct (15), and the luciferase activity was measured using luciferase detection reagent (Promega).

Western Blot, Immunoprecipitation, and Immunofluorescence—Isolation of total heart protein lysates and Western blot analysis were performed using a protocol described previously (16). For immunoprecipitation, protein extracts were precleared by incubation with Bio-Adembeads protein AG (Ademtech) for 2 h at room temperature. Beads were separated using a magnetic device. Precleared extracts were then incubated overnight with 5 μg of indicated antibody and 20 μl of Bio-Adembeads Protein AG. Beads were recovered using a magnetic device and washed three times with 500 μl of radioimmune precipitation assay buffer. Washed beads were resuspended in Laemmli loading buffer and analyzed by Western blot. Immunofluorescence analysis was conducted using a standard protocol as described previously (18).

Histology—Heart tissues were fixed in phosphate-buffered saline (PBS) containing 4% paraformaldehyde, embedded in paraffin, and then sectioned at 5-μm thickness. Hematoxylin and eosin and Masson's trichrome stainings were conducted using standard procedures.

Measurement of Cardiomyocyte Size and Myocardial Fibrosis—Cross-sectional cardiomyocyte size was measured on sections stained with hematoxylin and eosin using ImageJ software (NIH). We measured 50–100 cells from at least four different frames in each independent animal ($n = 6–8$ mice per group). Myocardial fibrosis was measured on Masson's trichrome stained sections. At least five randomly chosen frames from each animal ($n = 6–7$ mice per group) were analyzed.

TUNEL Assay—TUNEL assay to detect apoptosis was conducted on heart sections and cultured NRCM using the *in situ* Cell Death Detection kit (Roche Applied Science) following protocol recommended by the manufacturer. Triple staining with TUNEL, anti-α-actinin antibody (Sigma), and DAPI was performed to confirm apoptosis in myocyte nuclei.

RNA Isolation and Real time RT-PCR—Total RNA was prepared from isolated heart tissue using TRIzol reagent (Invitrogen) following the manufacturer's instructions. We used the QuantiTect-SYBR Green RT-PCR system (Qiagen) for real time quantitative RT-PCR analysis. Analysis of gene expression was performed using the $2^{\Delta\Delta Ct}$ method and are presented as fold induction of target gene transcripts relative to control. Reactions were performed in an ABI PRISM 7700 (Applied Biosystems). Primers were purchased from Qiagen (Quantitect Primer Assay system). Threshold cycle (*Ct*) values were determined using the Sequence Detection System software. GAPDH levels were used as a reference.

Antibodies—The primary antibody to detect Mst2 was obtained from Abgent. Antibodies for Mst1, ERK1/2, phospho-ERK1/2 (Thr^{202}/Tyr^{204}), phospho-Raf1 (Ser^{338}), phosphatase

2A-C, YAP1, and phospho-YAP1 (Ser^{127}) were obtained from Cell Signaling Technologies. Antibodies for Raf1 and GAPDH were obtained from Abcam. We used horseradish peroxidase-labeled secondary antibodies (Cell Signaling) for visualization. For immunofluorescence and immunohistochemistry, anti-α-actinin (Sigma), and anti Ser^{10} phospho-HH3 (Cell Signaling Technologies) were used. Anti Ki67 antibody (Abcam) and anti-phalloidin (Molecular Probes) were also used. We used Texas Red or FITC-labeled secondary antibodies (Jackson ImmunoResearch Laboratories) for visual detection.

Mitral Valve Prolapse Patients—We studied patients with clinically severe mitral regurgitation due to mitral valve prolapse. Patients with any other valvular diseases with the exception of mild tricuspid valve regurgitation were excluded. We also excluded patients with coronary artery disease, severe heart failure (New York Heart Association IV), uncontrolled hypertension (blood pressure >160/90 mmHg), significant respiratory disease, renal impairment (creatinine >150 mmol/liter) and peripheral vascular disease. Patients were recruited from the Cardiovascular Department at South Manchester University Hospital. The study protocol was approved by the local Research Ethics Committee, and all patients gave written informed consent. Symptoms were evaluated using the New York Heart Association Classification.

Echocardiography of Mitral Valve Prolapse Patients—All patients underwent trans-thoracic echocardiography and Doppler examination (Sonos 5500, Phillips Medical, Eindhoven, The Netherlands). All measurements were performed according to the American Society of Echocardiography guidelines (19). Regurgitant volume and fraction were measured using the volumetric method (20). Left ventricular mass was calculated using the Devereux method (21) and indexed to body surface area. Left ventricular volumes and ejection fraction were calculated using the modified Simpson's biplane method.

Polymorphism Detection—Genomic DNA was extracted from peripheral blood using the QIAamp DNA blood isolation kit (Qiagen). Polymorphisms were detected using TaqMan SNP genotyping assay (Applied Biosystems) following the protocol recommended by the manufacturer. Reactions were performed in an ABI PRISM 7700 real time PCR machine.

3′-UTR Assay—The ~1.2-kb 3′-UTR sequence of human *MST2* gene was PCR-amplified and inserted into the pMirGlo Dual-Luciferase vector (Promega) downstream of the luciferase gene. The effect of 3′-UTR sequence insertion was analyzed in primary human fibroblast cells (obtained from Invitrogen). 10^6 cells were cultured in 24-well plates in DMEM supplemented with 10% FBS. 2 μg of reporter construct was transfected using Lipofectamine 2000 reagent (Invitrogen) following the manufacturer's instructions. Luciferase activity was examined after 24 h of transfection. The *Renilla* luciferase activity was also examined for normalization of transfection efficiency.

Data Analysis—Data are expressed as mean ± S.E. and analyzed using the Student's *t* test or one-way analysis of variance followed by post hoc multiple comparison test where appropriate. A p value < 0.05 was considered significant.

RESULTS

Ablation of Mst2 Alone Did Not Alter Cell Proliferation in Mouse Heart—To investigate the role of Mst2 in the heart, we analyzed mice with genetic ablation of the *Mst2* gene ($Mst2^{-/-}$), which resulted in complete absence of this protein in the heart (Fig. 1*A*). Because inhibition of Hippo pathway in embryonic hearts resulted in increased cardiomyocyte proliferation (8), we therefore analyzed cardiomyocyte proliferation in $Mst2^{-/-}$ neonatal hearts. We examined hearts from 3-day-old WT and $Mst2^{-/-}$ neonates and stained them with markers of cell mitosis: phospho-Ser^{10} histone H3 (pHH3). We found that there was no difference in the level of pHH3-positive cells between WT and $Mst2^{-/-}$ neonates (Fig. 1, *B* and C). In addition, analysis of heart weight/body weight ratio (HW/BW) showed that there was no difference in cardiac size between WT and $Mst2^{-/-}$ neonates (Fig. 1*D*). We also examined pHH3 expression in adult hearts. We did not detect any cardiomyocytes positive for pHH3 expression in $Mst2^{-/-}$ or WT hearts (Fig. 1*E*). Consistently, HW/BW ratio was not different between $Mst2^{-/-}$ and WT adult hearts (Fig. 1*F*). As positive controls for this analysis, we performed pHH3 immunostaining in intestines (Fig. 1*G*). Taken together, our data indicated that genetic knock-out of *Mst2* did not alter cardiomyocyte proliferation in either newborn or adult heart.

Cardiac Mst2 Level Was Elevated in Pathological Conditions—To assess cardiac Mst2 expression level in pathological conditions, we subjected wild type mice to TAC to induce pressure overload. Two weeks after TAC treatment the heart weight/tibia length ratio was significantly increased (Fig. 2*A*). Western blot analysis showed that expression of Mst2 was elevated by ~2 folds (Fig. 2, *B* and *C*), suggesting that Mst2 may be involved in the regulation of pathological hypertrophy.

To assess whether Mst2 expression is also up-regulated in human heart failure, we analyzed *MST2* expression in failing human hearts. In keeping with the data from mouse model, the MST2 level was elevated by almost 2-fold in failing human hearts (Fig. 2*D*), further emphasizing the importance of this protein during pathological processes.

To determine the cell specificity, we examined *Mst2* expression in cardiomyocytes and cardiofibroblasts isolated from rat neonatal hearts. Using immunofluorescence, we found that MST2 was present in both cell types (Fig. 2*E*). Moreover, in response to phenylephrine treatment (20 μM, 48 h), there was a trend of increased Mst2 expression in cardiomyocytes by ~1.5 fold ($p = 0.09$, Fig. 2*F*).

Genetic Ablation of Mst2 Reduced Pathological Hypertrophy and Fibrosis in Response to Pressure Overload—To further study the role of Mst2 in pathological condition, we subjected $Mst2^{-/-}$ mice to TAC for 2 weeks. $Mst2^{-/-}$ mice showed a significantly less hypertrophic response compared with WT littermates (~30% increased of heart weight/tibia length ratio in $Mst2^{-/-}$ *versus* ~50% increase in WT, Fig. 3, *A* and *B*). Furthermore, the expression of hypertrophic markers such as BNP and atrial natriuretic peptide were significantly lower in $Mst2^{-/-}$ mice compared with wild type following TAC (Fig. 3, *C* and *D*).

Consistently, analysis of histological sections revealed less cardiac remodeling in $Mst2^{-/-}$ mice. Two weeks after TAC, we

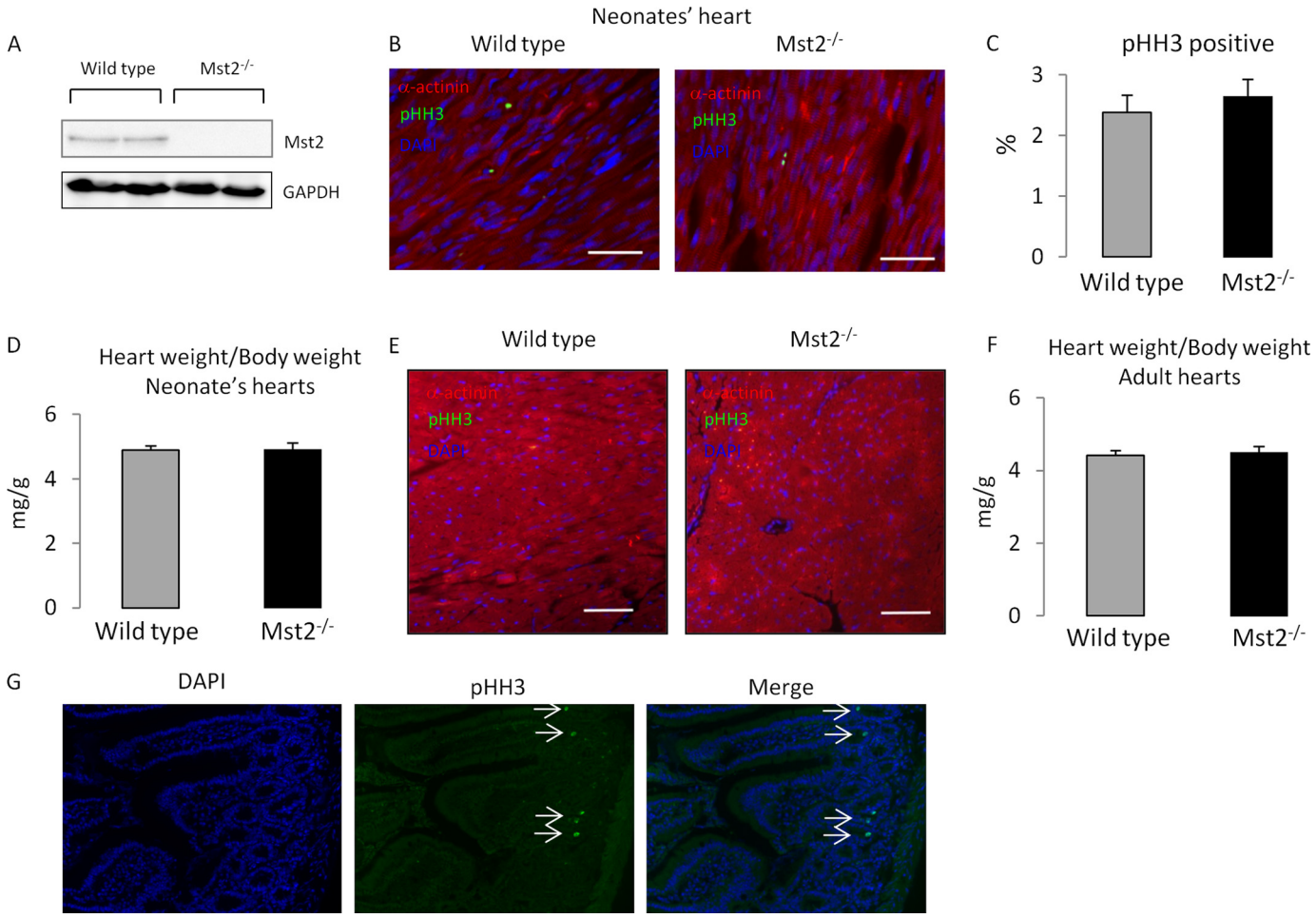

FIGURE 1. **Analysis of cardiomyocyte proliferation in *Mst2*$^{-/-}$ hearts.** *A*, expression of *MST2* was completely ablated in *Mst2*$^{-/-}$ hearts as indicated by Western blot. *B*, immunostaining of heart sections from WT and *Mst2*$^{-/-}$ neonates (3 days of age). Sections were stained with anti-α-actinin (*red*), anti-phospho-HH3 (*green*), and DAPI (*blue*) (*scale bars*, 50 μm). *C*, no difference in the number of pHH3-positive cells between WT and *Mst2*$^{-/-}$ neonates was observed. *D*, quantification of heart weight/body weight ratio showed that there was no difference in cardiac size between WT and *Mst2*$^{-/-}$ neonate hearts. *E*, immunostaining of heart sections from WT and *Mst2*$^{-/-}$ mice stained with anti-α-actinin (*red*), anti-phospho-HH3 (*green*), and DAPI (*blue*) (*scale bars*, 50 μm). *F*, heart weight/body weight ratio was not different between WT and *Mst2*$^{-/-}$ adult mice. *G*, immunofluorescence analysis using pHH3 antibody in small intestine sections as positive control of this assay. The results showed that pHH3 staining was able to detect proliferating cells (*arrows* indicate pHH3-positive cells).

found that the cardiomyocyte cross-sectional area was significantly smaller in *Mst2*$^{-/-}$ mice compared with WT littermates (Fig. 3, *E* and *F*). Equally important, *Mst2*$^{-/-}$ mice also displayed significantly less cardiac fibrosis as indicated by Masson's trichrome staining and the level of collagen 1 and 3 expression (Fig. 3, *G–J*). Together, these data suggest a key role of Mst2 during pathological hypertrophy and cardiac remodeling.

Echocardiographic assessment revealed that the ventricular wall thickness of *Mst2*$^{-/-}$ mice was significantly thinner compared with WT following TAC (Fig. 4*A*). In addition, *Mst2*$^{-/-}$ mice displayed smaller left ventricular (LV) end diastolic dimension and lower LV mass/body weight ratio after TAC (Fig. 4, *B* and *C*). These data support the finding that *Mst2*$^{-/-}$ displayed a reduced hypertrophic response. However, no difference in ejection fraction was observed between WT and *Mst2*$^{-/-}$ mice (Fig. 4*D*).

Using a pressure-volume system, we examined the hemodynamic parameters such as dP/dt max, dP/dt min, and end systolic pressure volume relationship. We did not observe any difference in all the contractility parameters tested between WT and *Mst2*$^{-/-}$ mice, suggesting that there was no alteration in cardiac function in both groups of mice after 2 weeks of TAC (Fig. 4, *E–G*). It is important to note that the left ventricular systolic pressure was not different between *Mst2*$^{-/-}$ and WT after TAC, suggesting a similar degree of pressure overload between these groups (Fig. 4*H*).

Apoptosis Level—In non-cardiac cells, Mst2 has been described as an important regulator of apoptosis (22). We therefore analyzed apoptosis level in the hearts following TAC. We observed a reduction in the number of apoptotic nuclei in *Mst2*$^{-/-}$ mice after TAC compared with controls as indicated by TUNEL staining (Fig. 5, *A* and *B*). These data are consistent with previous reports which showed that Mst1, the isoform of Mst2, is a positive modulator of apoptosis (11, 12).

To further investigate the role of Mst2 in cardiomyocytes, we generated an adenovirus to overexpress Mst2 in NRCM (Fig. 5*C*). Using TUNEL assay, we found a consistent data with the *in vivo* observation, in which NRCM overexpression resulted in higher level of apoptosis in NRCM (Fig. 5, *D* and *E*).

Fibroblast Proliferation Rate—Fibroblasts play an important role during cardiac remodeling and fibrosis. Because there was

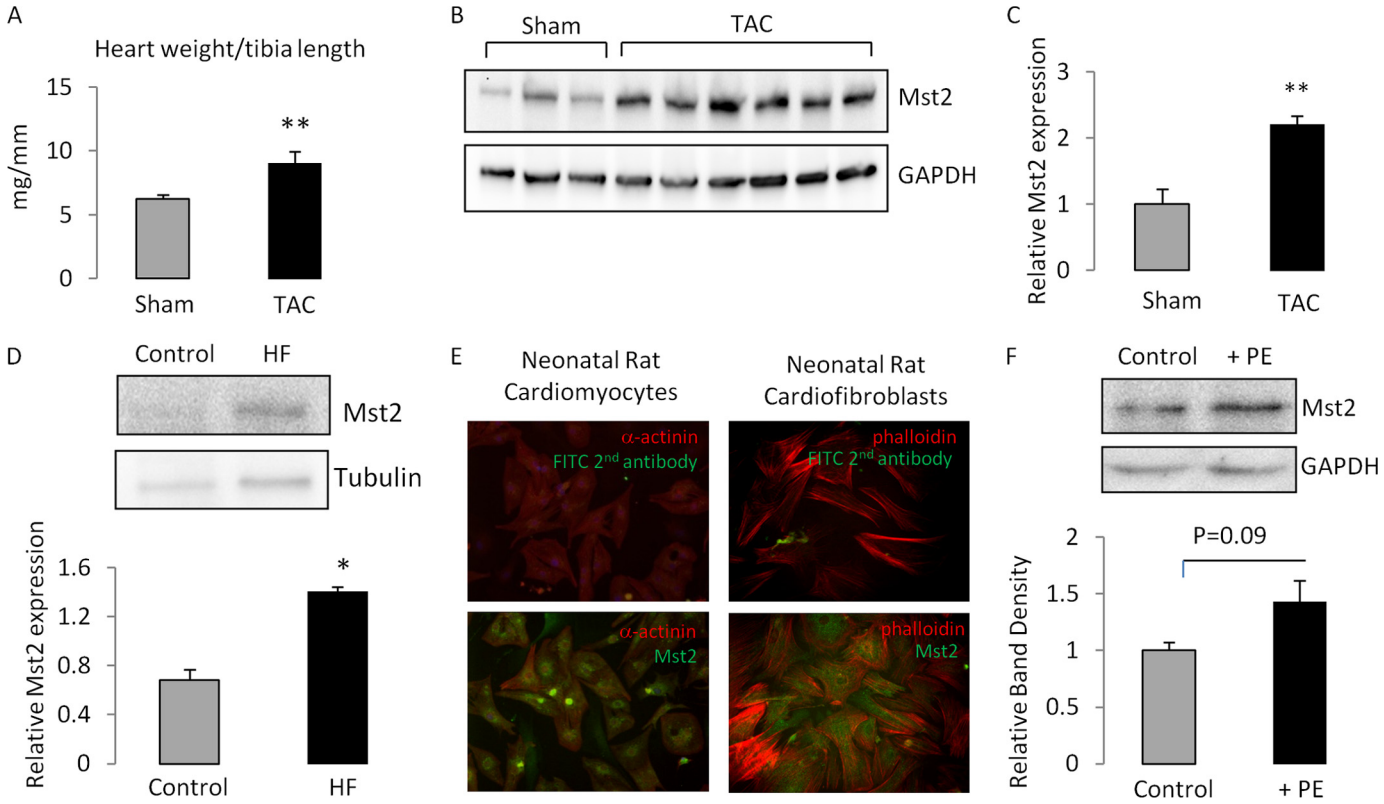

FIGURE 2. **Cardiac expression of MST2 in pathological conditions.** *A*, wild type mice were subjected to TAC to induce pressure overload cardiac hypertrophy. Heart weight/tibia length ratio was significantly increased in the TAC group ($n = 5$–10 in each group; **, $p < 0.01$ *versus* sham). *B*, Western blot analysis of *Mst2* expression in mouse heart lysates following TAC or sham operation. *C*, analysis of band density showed a significant increase in MST2 level in hypertrophic hearts ($n = 5$;**, $p < 0.01$). *D*, MST2 expression in humans with end-stage heart failure (*HF*) was detected by Western blot. Quantification of band density showed that MST2 level was elevated in failing hearts ($n = 3$ in each group; *, $p < 0.05$). *E*, immunofluorescence analysis of MST2 expression in cardiomyocytes and cardiofibroblasts isolated from rat neonatal hearts. *F*, Westen blot and band density quantification of MST2 expression in neonatal rat cardiomyocytes following phenylephrine (*PE*) treatment (20 μM, 48 h). *Con*, control.

a significant difference in the level of fibrosis between WT and *Mst2*$^{-/-}$ mice, it is important to analyze whether fibroblasts proliferation rate is different between these mice. We isolated adult cardiac fibroblasts from WT and *Mst2*$^{-/-}$ and performed Ki67 staining (marker of mitosis) and BrdU incorporation assay. Results shown in Fig. 6, *A–D*, suggested that there was no difference in proliferation rate between WT and *Mst2*$^{-/-}$ adult cardiac fibroblasts.

Cellular Mechanisms of Mst2 Mediated Raf1/ERK1/2 Regulation—Mst2 has been described previously to form a molecular interaction with Raf1 in COS-1 cells (23). Raf1 is an important progrowth and survival kinase that modulates the mitogen-activated protein kinase (MAPK) pathway (24). We therefore examined whether Mst2 interacts and modulates Raf1 in cardiomyocytes. Immunoprecipitation analyses in isolated cardiomyocytes (Fig. 7*A*) and mouse whole heart lysates (Fig. 7*B*) showed that Mst2 and Raf1 were co-immunoprecipitated, strongly suggesting a physical interaction between these molecules.

To further analyze the regulatory mechanism of the Mst2-Raf1 signaling complex in cardiomyocytes, we generated an adenovirus expressing inactive mutant form of Mst2 (Mst2 K56R mutant) (17). As shown in Fig. 7, *C–E*, overexpression of wild type Mst2 enhanced the level of Raf1 phosphorylation in cardiomyocytes. We also detected increased phosphorylation of prohypertrophic kinase ERK1/2, which is a downstream effector of Raf1. In contrast, Mst2 K56R mutant overexpression failed to induce phosphorylation of Raf1 and ERK1/2, suggesting that the kinase activity of Mst2 is likely to be responsible for the activation of Raf1 and ERK1/2.

To investigate the importance of Mst2-Raf1 interaction, we generated Mst2 truncation mutant. We generated adenovirus expressing Mst2-ΔC (containing amino acid residues 1–277) by deletion of amino acids 288–491 and removing the Salvador RASSF Hippo (SARAH) domain at the C terminus region of Mst2. Expression of this mutant molecule was detected by Western blot (Fig. 7*F*). The immunoprecipitation experiment showed that this molecule did not interact with Raf1 in cardiomyocytes (Fig. 7*G*). Surprisingly, when we overexpressed Mst2-ΔC in NRCM, we still found increased level of ERK1/2 phosphorylation which was comparable with those of Mst2 WT-overexpressing cells (Fig. 7*H*). This data suggested that protein interaction between Mst2-Raf1 was not necessary in the regulation of Raf1/ERK1/2 by Mst2.

Previously, it has been reported that Mst2 positively regulated Raf1 through modulation of phosphatase 2A (PP2A) (25). Therefore, we examined the expression of the catalytic C subunit of PP2A in NRCM-overexpressing Mst2. We found a trend of increased PP2A-C in Mst2-overexpressing cardiomyocytes (Fig. 7, *I–J*), which is consistent with previously published observations (25). This indicates that PP2A might be involved in Mst2-dependent regulation of Raf1/ERK1/2 in cardiomyocytes.

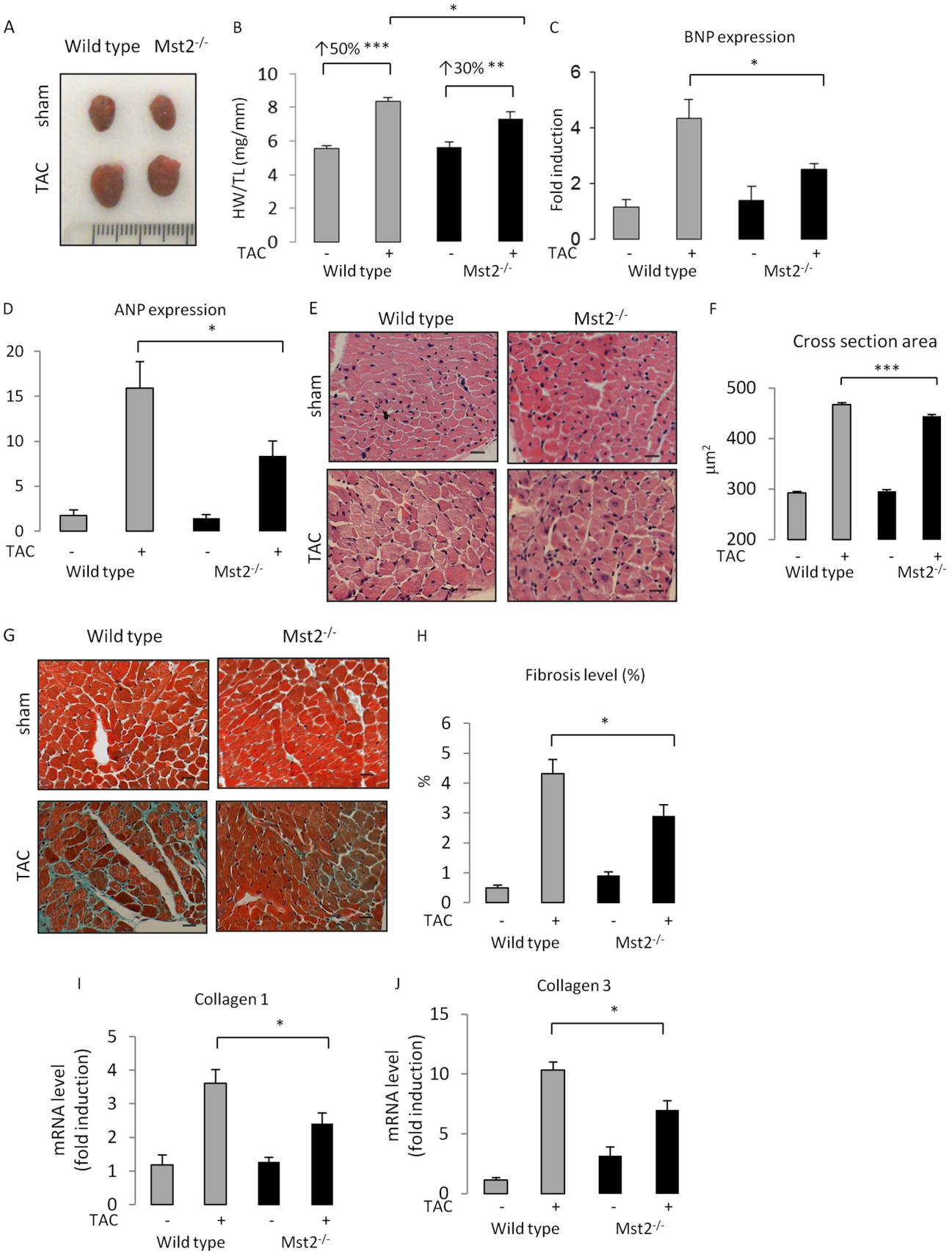

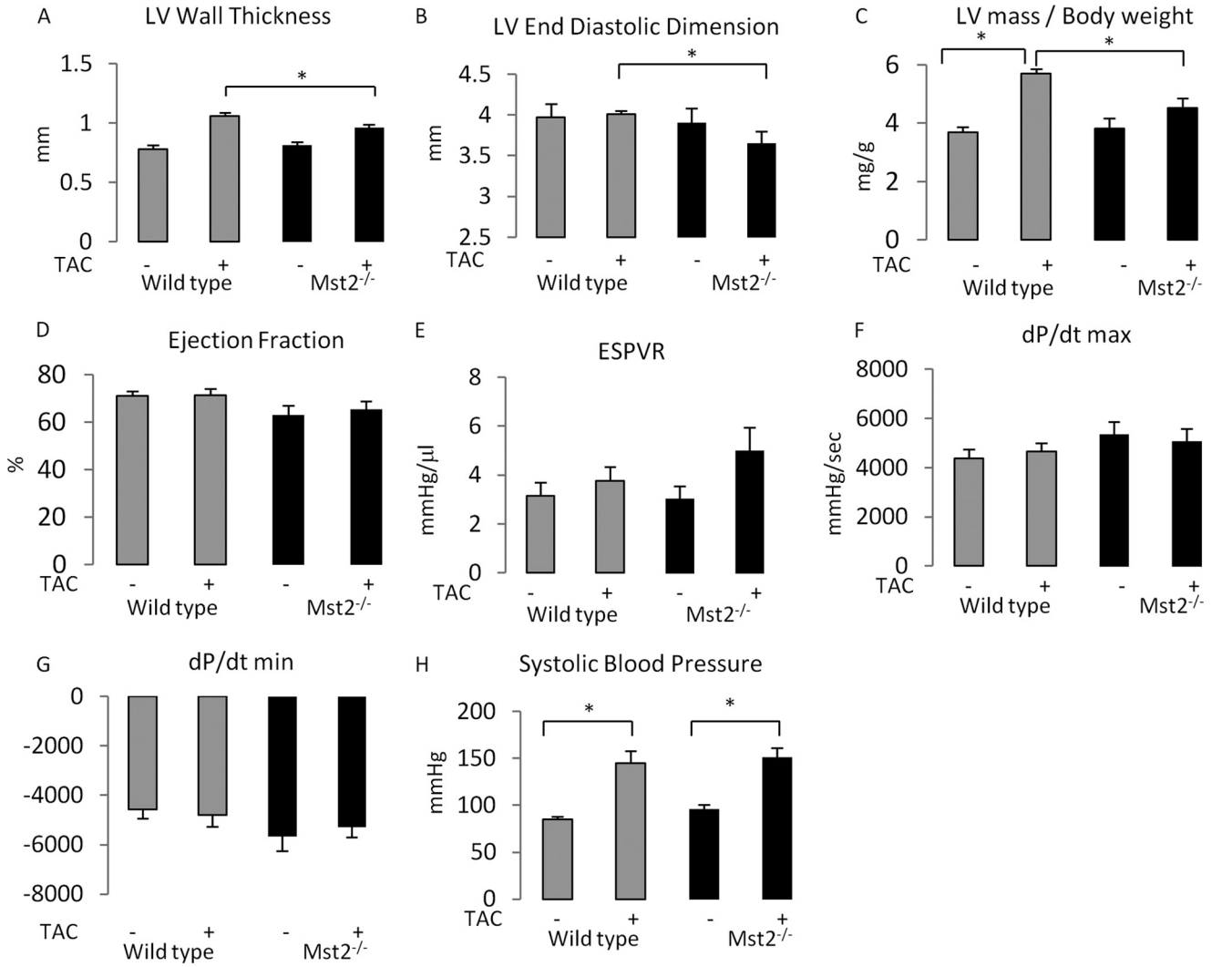

FIGURE 4. **Echocardiography and hemodynamic analysis.** Ventricular wall thickness (average of posterior and interventricular septum wall thickness) (*A*) and left ventricular end diastolic diameter (*B*) in $Mst2^{-/-}$ mice compared with WT after TAC or sham operation ($n = 7–8$; *, $p < 0.05$). *C*, left ventricular mass/body weight ratio was significantly higher in WT mice ($n = 7–8$; *, $p < 0.05$). However, there were no differences in cardiac contractility indices as indicated by *D*. End systolic pressure volume relationship (*ESPVR*), ejection fraction (*E*), dP/dt max (*F*), and dP/dt min (*G*). *H*, left ventricular systolic pressure was significantly elevated following TAC in both genotypes; however, no difference between WT and knock-out was observed basally or after TAC.

Mst2 Overexpression Enhanced Phenylephrine-induced Cardiomyocyte Hypertrophy—We performed an *in vitro* model of cardiomyocyte hypertrophy by treating NRCM with phenylephrine (20 μM, 48 h). Mst2 overexpression significantly enhanced cardiomyocyte size basally by ~19% and increased phenylephrine-induced cardiomyocyte hypertrophy from ~30% in control to ~42% in Mst2-overexpressing cells as indicated by cell surface area measurements (Fig. 8, *A* and *B*). Moreover, using an adenovirus mediated BNP-luciferase reporter construct, we also detected significantly higher expression of the hypertrophic marker BNP in Mst2-overexpressing cells (Fig. 8*C*).

To ascertain that the Mst2 prohypertrophic action was through regulation of the ERK1/2 pathway, we treated cardiomyocytes overexpressing Mst2 with ERK1/2-specific inhibitor FR180204. This inhibitor has been shown to have a potent and specific inhibition of ERK1 (IC_{50} = 510 nM) and ERK2 (IC_{50} = 330 nM) (26). As shown in Fig. 8, *B* and *C*, inhibition of ERK1/2 reduced the hypertrophic response of Mst2-overexpressing myocytes to the level comparable with control cells, strongly indicated the implication of ERK1/2 in this process.

We then analyzed the effect of expressing Mst2 K56R mutant. Cell size analysis showed that overexpression of Mst2 K56R mutant significantly reduced cardiomyocyte size at basal

FIGURE 3. ***In vivo* model of pressure overload induced hypertrophy in $Mst2^{-/-}$ mice.** *A*, hearts from WT and $Mst2^{-/-}$ mice following TAC (2 weeks) or sham operation. *B*, analysis of HW/tibia length ratio showed significant reduction of hypertrophic response in $Mst2^{-/-}$ mice ($n = 7–8$ in each group; *, $p < 0.05$; **, $p < 0.01$; ***, $p < 0.001$). Expression of hypertrophic markers were as follows: BNP (*C*) and atrial natriuretic peptide (*ANP*; *D*) were detected using real time RT-PCR. Values indicate fold change of expression after normalization with GAPDH level ($n = 5–7$ in each group; *, $p < 0.05$). Histological sections stained with hematoxylin and eosin (*E*) and quantification of cardiomyocyte cross-sectional area (*F*) showed smaller cardiomyocyte size in $Mst2^{-/-}$ mice after TAC (*scale bars*, 20 μm; ***, $p < 0.001$). Masson's trichrome staining (*G*) and quantification of fibrotic area (*H*) indicated significantly less fibrosis in $Mst2^{-/-}$ mice (*, $p < 0.05$). Expressions of collagen 1 (*I*) and collagen 3 (*J*) were detected using real time RT-PCR. Values indicate fold change of expression following normalization with GAPDH level ($n = 5–7$ in each group; *, $p < 0.05$).

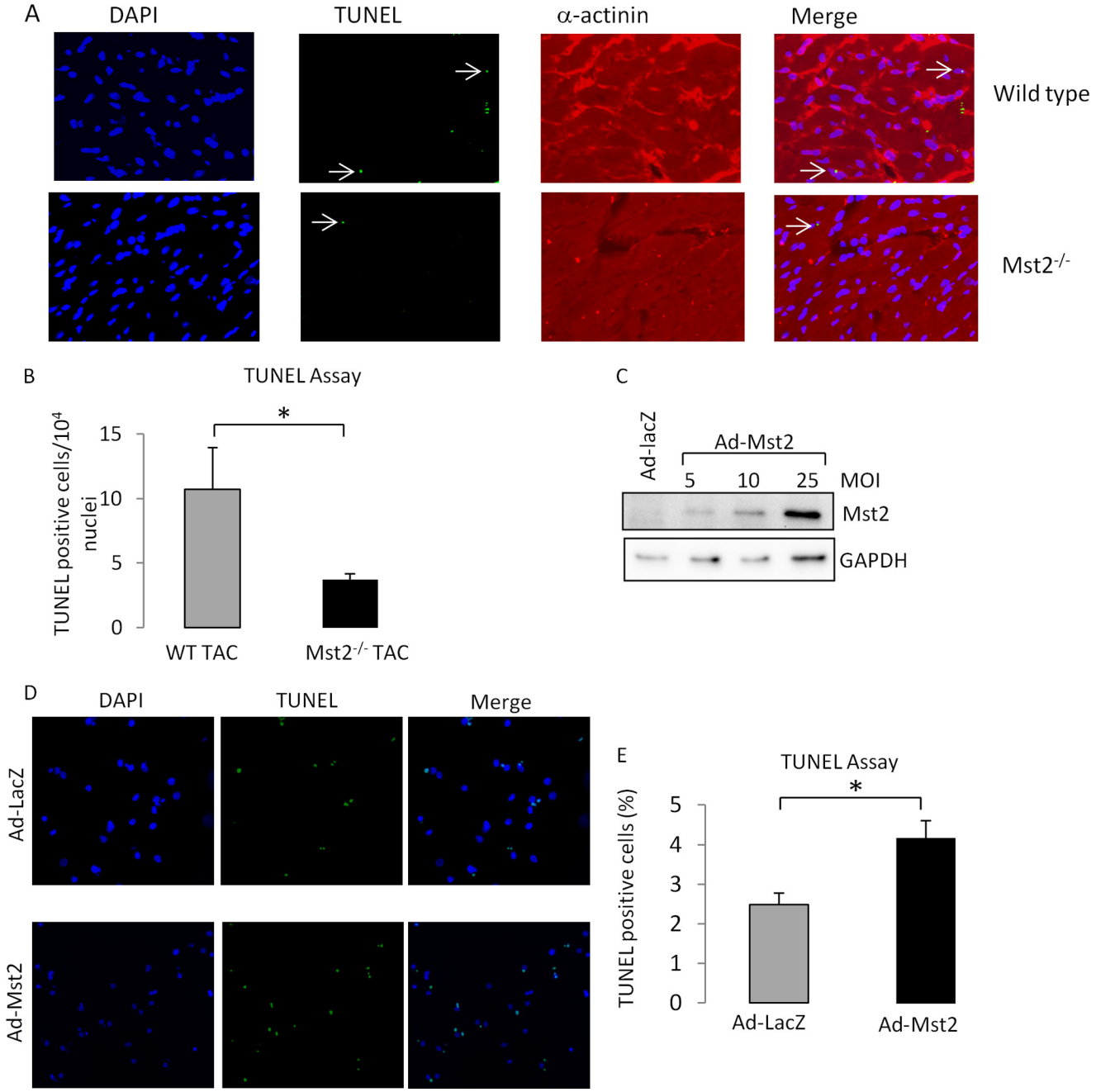

FIGURE 5. **Detection of apoptotic cells in *Mst2*$^{-/-}$ hearts and in isolated cardiomyocytes overexpressing Mst2.** *A*, examples of TUNEL staining to detect apoptotic cells. Triple staining was performed: TUNEL (*green*), DAPI (*blue*), and α-actinin (*red*). *Arrows* indicate TUNEL-positive nuclei. *B*, calculation of TUNEL-positive nuclei revealed that *Mst2*$^{-/-}$ mice exhibited a reduced level of apoptosis compared with WT following TAC ($n = 4–5$; *, $p < 0.05$). *C*, immunoblot analysis showing dose-dependent expression of Mst2 in NRCM following infection with adenovirus expressing human Mst2 (*Ad-Mst2*). Adenovirus expressing LacZ (*Ad-LacZ*) was used as a control. (*MOI*, multiplicity of infection). *D*, representatives TUNEL staining in neonatal rat cardiomyocytes treated with adenovirus expressing Mst2 or LacZ (control). *E*, quantification of TUNEL-positive nuclei showed more apoptotic cells in cardiomyocytes expressing Mst2 (*, $p < 0.05$).

condition by ~15%. Interestingly, there was no difference in the hypertrophic response against phenylephrine stimulation (Fig. 8*D*).

Mst2 Modulated Raf1-ERK1/2 Pathway in Pathological Conditions—Our cellular model showed that in cardiomyocytes Mst2 was linked to the prohypertrophic MAPK pathway via Raf1. However, Mst2 has been widely known as a central component of the Hippo signaling pathway (5). We therefore focused on these two pathways to uncover the molecular mechanism responsible for the reduce response to hypertrophic stress observed in *Mst2*$^{-/-}$ mice.

Our data presented in Fig. 9 indicated that the MAPK pathway was modulated by Mst2. We investigated whether Mst2 modulates Raf1 following pathological stress. Western blot analysis showed that Raf1 phosphorylation was significantly reduced in *Mst2*$^{-/-}$ compared with WT following TAC (Fig. 9, *A* and *B*). Because Raf1 is an upstream activator of the prohypertrophic kinase ERK1/2 (24, 27), we also examined activa-

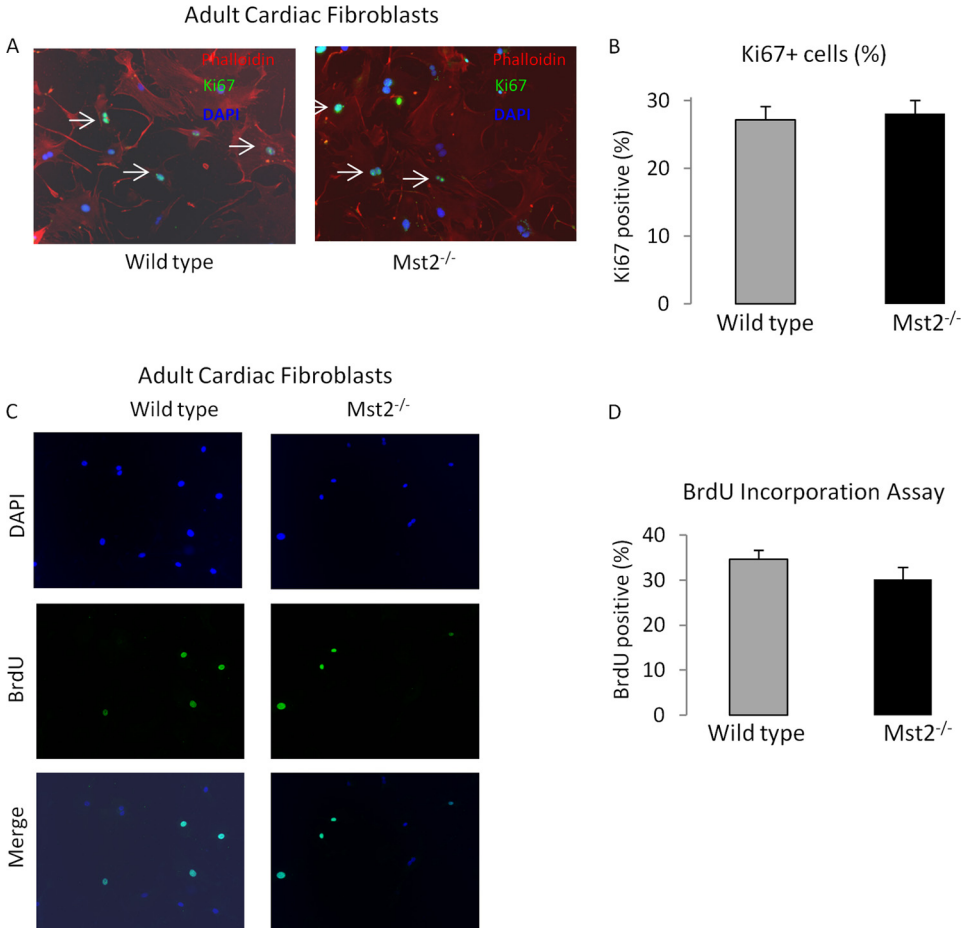

FIGURE 6. **Analysis of adult cardiac fibroblast proliferation rate.** Adult cardiac fibroblasts were isolated from *Mst2*$^{-/-}$ and WT littermates. *A*, immunostaining with mitosis marker Ki67. *Arrows* indicate Ki67-positive nuclei. *B*, quantification of Ki67-positive cells showed that there was no difference between WT and *Mst2*$^{-/-}$ cardiac fibroblasts. *C*, fibroblasts were treated with 1:100 dilution of BrdU-labeling reagent (Invitrogen) for 24 h, and the presence of BrdU-positive cells was determined by immunostaining. *D*, quantification of BrdU-positive cells supported the Ki67 staining data that there was no difference in the proliferation rate between WT and *Mst2*$^{-/-}$ cardiac fibroblasts.

tion of these kinases by Western blot. Data presented in Fig. 9, *A* and *C*, showed that ablation of Mst2 significantly reduced phosphorylation of ERK1/2 following TAC.

YAP Activation Was Not Affected in Mst$^{-/-}$ *Hearts Following TAC*—We then analyzed whether the Hippo signaling pathway was differently regulated in Mst2-deficient mice. Mst1 expression was elevated following TAC; however, no difference was observed between WT and *Mst2*$^{-/-}$ mice (Fig. 10, *A* and *B*). Consistently, we observed similar levels of YAP phosphorylation in post-TAC heart tissue lysates between KO and WT (Fig. 10*C*). YAP is known as the downstream effector of Mst1/2 and the major components of the Hippo pathway. Therefore, these results suggest that in adult cardiac cells Mst2 ablation did not affect the activation of YAP following stress.

A Polymorphism in the Human MST2 Gene Was Associated with Adverse Left Ventricular Remodeling in Mitral Valve Prolapse Patients—We conducted an initial study to investigate whether genetic variation in the human *MST2* gene is associated with cardiac remodeling in patients with mitral valve prolapse. We analyzed single nucleotide polymorphisms (SNPs) in the human *MST2* gene in 62 mitral valve prolapse patients. Based on sequence analysis, we focused our study on two SNPs located in the regulatory region of the human *MST2* gene: (i) rs3019294, which is located at the promoter region and may affect the binding of transcription factors; ii) rs10955176, which is located at the 3′-untranslated region (3′-UTR) sequence and may interfere with the binding of human micro RNAs. Although we found no association between rs3019294 with all parameters tested (Table 1), we did identify that rs10955176 was significantly associated with hypertrophic parameters such as LV mass and wall thickness (Table 2). This SNP is an A-to-G substitution located 214 base pairs downstream of the stop codon; therefore, we refer to this SNP as +214A/G polymorphism. Patients carrying the GG allele showed greater LV mass and wall thickness, despite similar level in the indices of mitral regurgitation and LV function.

To investigate whether this SNP regulates gene expression, we isolated the whole 3′-UTR sequence (~1.2 kb) from patients carrying the GG or AA allele and cloned them into a luciferase-based reporter cassette (Fig. 11*A*). Expression of *Renilla* luciferase driven by a constitutively active promoter within the same construct was used to control transfection efficiency. In primary human skin fibroblasts, we found that the reporter construct carrying the +214G 3′-UTR produced significantly higher luciferase signal than that carrying the +214A 3′-UTR

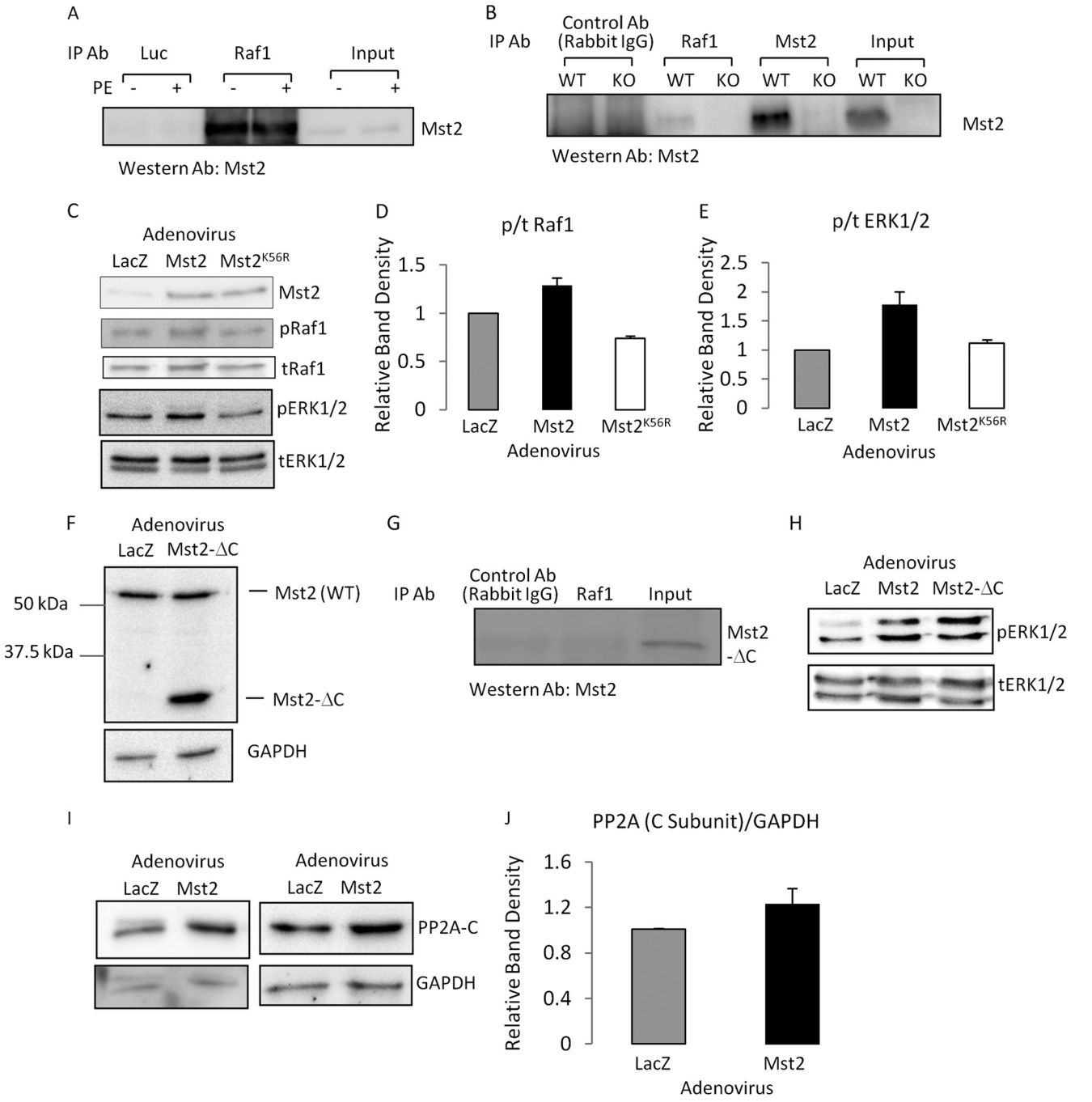

FIGURE 7. **Mst2 regulates Raf1 and ERK1/2 activation.** *A*, immunoprecipitation analysis of lysates from NRCM using Raf1 or control (*luc*, luciferase) antibody (*Ab*). Raf1 interacted with Mst2 in NRCM, but no difference in the amount of interacting protein was detected following phenylephrine (*PE*) stimulation. *B*, consistently, immunoprecipitation analysis of total heart lysates from WT and *Mst2*$^{-/-}$ showed that Mst2 was co-precipitated with Raf1. *C*, immunoblot analysis to detect phosphorylated/total Raf1 and phosphorylated/total ERK1/2 in NRCM overexpressing LacZ (control), Mst2, or Mst2 kinase-defective mutant (Mst2 K56R). Band density quantification of phospho-Raf1/total Raf1 (*D*) and phospho-ERK1/2/total ERK1/2 (*E*) (*, $p < 0.05$; $n = 3–4$ independent experiments). *E*, Western blot analysis showing the expression of truncated mutant Mst2-ΔC. *F*, immunoprecipitation analysis using Raf1 or control antibody in NRCM overexpressing Mst2-ΔC showed that mutant Mst2-ΔC did not interact with Raf1. *G*, overexpression of mutant Mst2-ΔC enhanced the level of phospho/total ERK1/2. *H*, representative immunoblots for the detection of PP2A C subunit in NRCM. *I*, densitometric analysis showed a trend of higher PP2AC level in NRCM overexpressing Mst2.

(Fig. 11*B*). This suggests that patients carrying the GG genotype may have more Mst2 expression.

DISCUSSION

This study demonstrates that Mst2 plays a key role in mediating stress-induced pathological hypertrophy and remodeling in the adult heart. Mice with genetic deletion of the Mst2 gene displayed a significant reduction in cardiac hypertrophy, apoptosis, and fibrotic remodeling following pressure overload. Conversely, overexpression of Mst2 in cardiomyocytes enhanced adrenergic-induced cardiomyocyte hypertrophy and fetal gene activation.

Interestingly, in our model, the ablation of Mst2 did not alter activation of YAP and hence cardiomyocyte proliferation. One possible explanation is that in the absence of Mst2, Mst1 con-

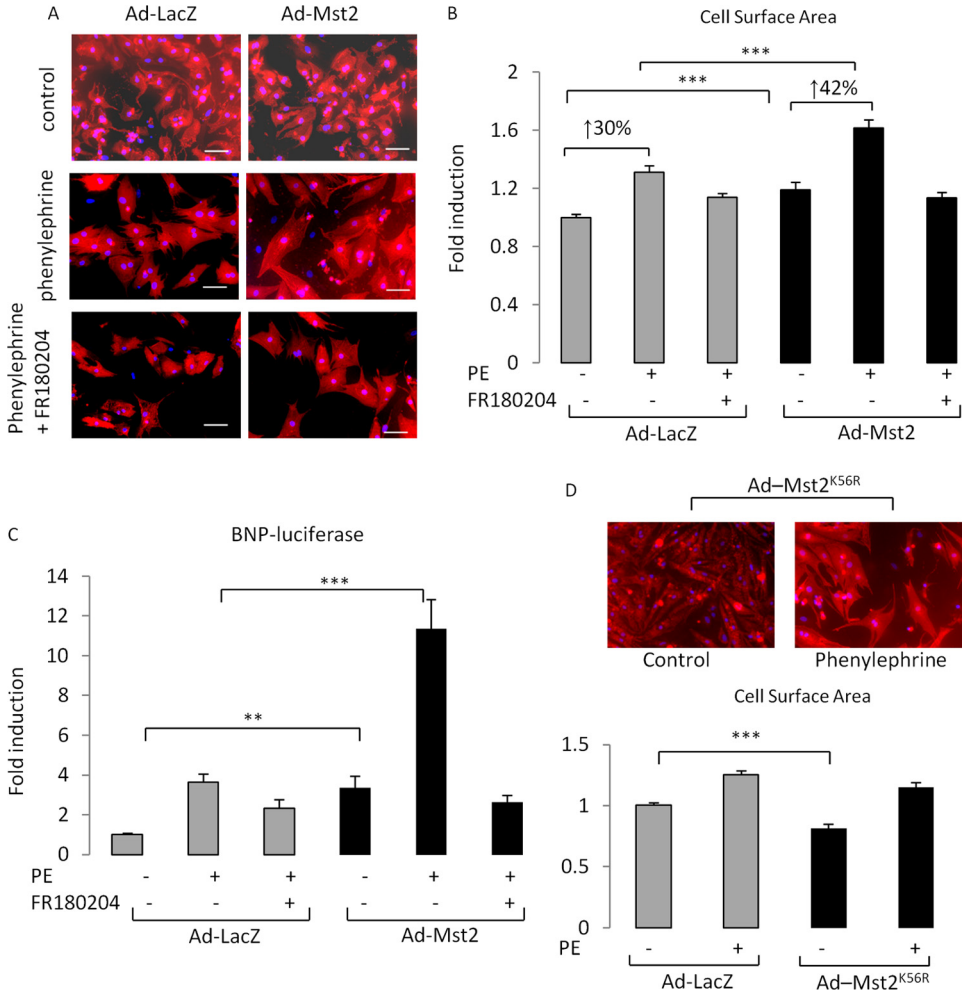

FIGURE 8. **Phenylephrine-induced cardiomyocyte hypertrophy model.** *A*, images of NRCM overexpressing Mst2 and control (LacZ) following treatment with 20 μM phenylephrine (*PE*) for 48 h with or without the addition of ERK1/2 inhibitor FR180204 (50 μM). Cells were stained with α-actinin antibody to specifically visualize cardiomyocytes. *Scale bars*, 50 μm. *B*, quantification of cell surface area indicated that Mst2 overexpression significantly enhanced phenylephrine-induced hypertrophic response. (Results were from four independent experiments conducted in triplicate; a minimum of 100 cells were measured per replicate.) (***, $p < 0.001$). Treatment with FR180204 reduced the hypertrophic response in Mst2-overexpressing cells to the level comparable with control cells with the same treatment. *C*, using adenovirus expressing a luciferase reporter driven by the rat BNP promoter, we found that Mst2 overexpression increased activation of the BNP promoter both basally and after phenylephrine stimulation ($n = 8$; **, $p < 0.01$;***, $p < 0.001$). Consistently, treatment with FR180204 abolished the difference in hypertrophic response between Mst2-overexpressing myocytes and control cells. *D*, representative images of NRCM-overexpressing Mst2 K56R mutant and the quantification of cell surface area at basal condition and after stimulation with phenylephrine (***, $p < 0.001$).

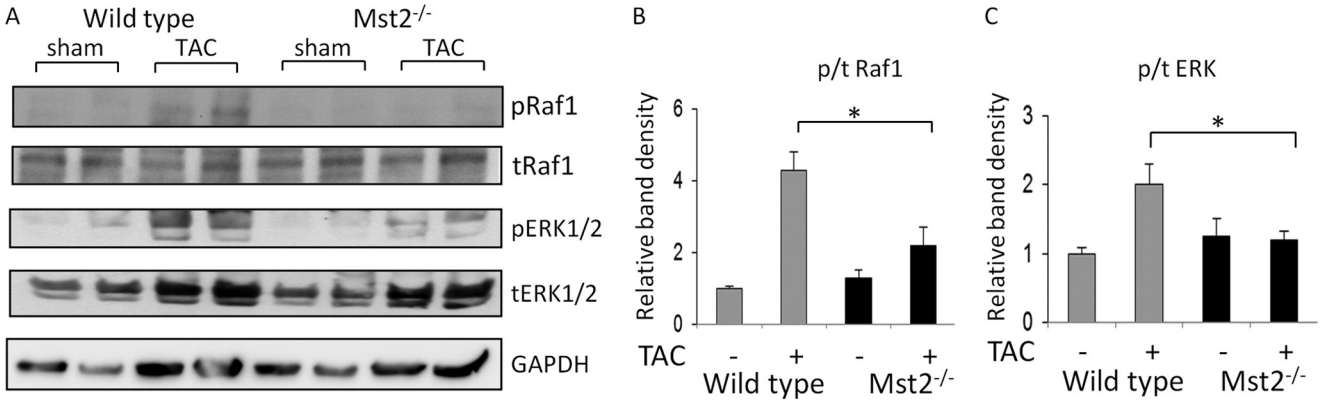

FIGURE 9. **Analysis of Raf1 and ERK1/2 activation during TAC-induced hypertrophy.** *A*, representative Western blots to detect phosphorylated/total Raf1 and phosphorylated/total ERK1/2 in total heart extracts of *Mst2*$^{-/-}$ and WT mice following TAC. Quantification of phosphorylated/total Raf1 (*B*) and ERK1/2 (*C*) showed that activation of Raf1 and ERK1/2 were decreased in *Mst2*$^{-/-}$ mice during pathological hypertrophy (*, $p < 0.05$; $n = 5$–7 in each group).

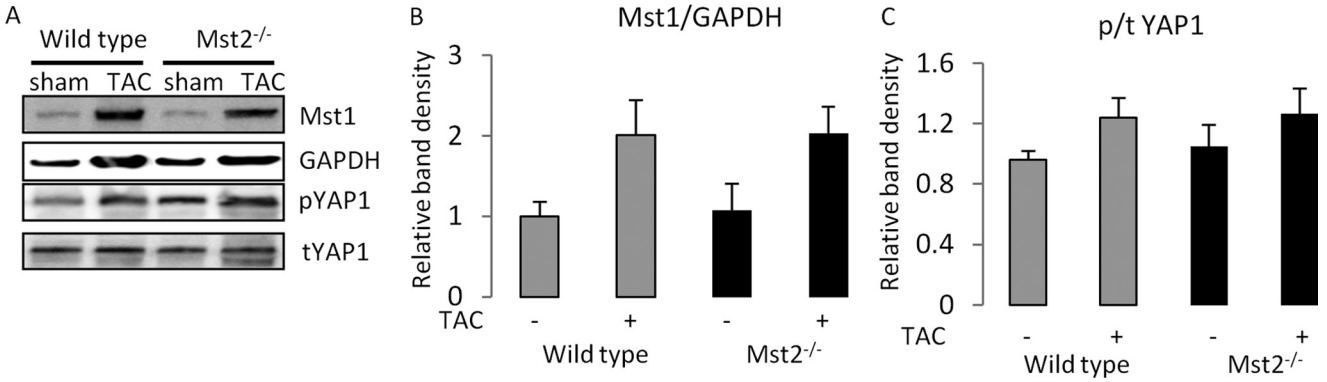

FIGURE 10. **Analysis of Mst1 expression and YAP activation in the hearts during hypertrophy.** *A*, immunoblot analyses to determine the level of MST1 and phosphorylated/total YAP (*tYAP*). Band density quantification of MST1 normalized to GAPDH level (*B*) and phosphorylated/total YAP (*C*) showed that the level of Mst1 expression as well as activation of YAP were not altered in *Mst2*$^{-/-}$ mice following TAC (n = 5–7 in each group).

TABLE 1

Characteristics of MVP patients according to rs3019294 polymorphism

LV, left ventricular; dPW, posterior wall thickness at diastole; sPW, posterior wall thickness at systole; dIVS, interventricular septal wall thickness at diastole; sIVS, interventricular septal wall thickness at systole. None of the differences are statistically significant.

Variable	CC	CT/TT
N	50	12
Gender (male/%)	34 (68%)	10 (83%)
Age (years)	63 ± 1.3	64 ± 3.0
Body mass index	25.4 ± 0.41	25.7 ± 0.92
Body surface area (m^2)	1.83 ± 0.02	1.88 ± 0.06
Systolic blood pressure (mmHg)	133 ± 1.3	138 ± 2.34
Diastolic blood pressure (mmHg)	76 ± 1.0	74 ± 2.2
LV end diastolic dimension (cm)	5.47 ± 0.10	5.36 ± 0.26
LV mass (g)	256 ± 13	278 ± 32
LV mass index (g/m^2)	139 ± 6.5	150 ± 19
dPW (cm)	1.15 ± 0.03	1.23 ± 0.07
sPW (cm)	1.54 ± 0.04	1.57 ± 0.10
dIVS (cm)	1.13 ± 0.04	1.24 ± 0.08
sIVS (cm)	1.60 ± 0.05	1.75 ± 0.10
Ejection fraction (%)	63 ± 0.9	61 ± 2.4
Regurgitation fraction (%)	64 ± 1.5	63 ± 3.6

TABLE 2

Characteristics of MVP patients according to *MST2* + 214 G/A (rs10955176) polymorphism

LV, left ventricular; dPW, posterior wall thickness at diastole; sPW, posterior wall thickness at systole; dIVS, interventricular septal wall thickness at diastole; sIVS, interventricular septal wall thickness at systole.

Variable	+214 GG	+214 GA/AA
N	16	46
Gender (male/%)	13 (81%)	31 (67%)
Age (years)	63 ± 1.9	63 ± 1.5
Body mass index	25.5 ± 0.68	25.4 ± 0.45
Body surface area (m^2)	1.88 ± 0.03	1.83 ± 0.03
Systolic blood pressure (mmHg)	137 ± 1.9	133 ± 1.4
Diastolic blood pressure (mmHg)	76 ± 1.8	75 ± 1.0
LV End diastolic dimension (cm)	5.70 ± 0.18	5.34 ± 0.11
LV mass (g)	306 ± 24	244 ± 13[a]
LV mass index (g/m^2)	164 ± 13.8	133 ± 6.8[a]
dPW (cm)	1.31 ± 0.06	1.11 ± 0.03[a]
sPW (cm)	1.73 ± 0.05	1.49 ± 0.04[a]
dIVS (cm)	1.21 ± 0.07	1.13 ± 0.04
sIVS (cm)	1.80 ± 0.09	1.58 ± 0.05[b]
Ejection fraction (%)	61 ± 2.3	63 ± 0.9
Regurgitant fraction (%)	65 ± 3.1	63 ± 1.6

[a] $p < 0.05$.
[b] $p = 0.05$.

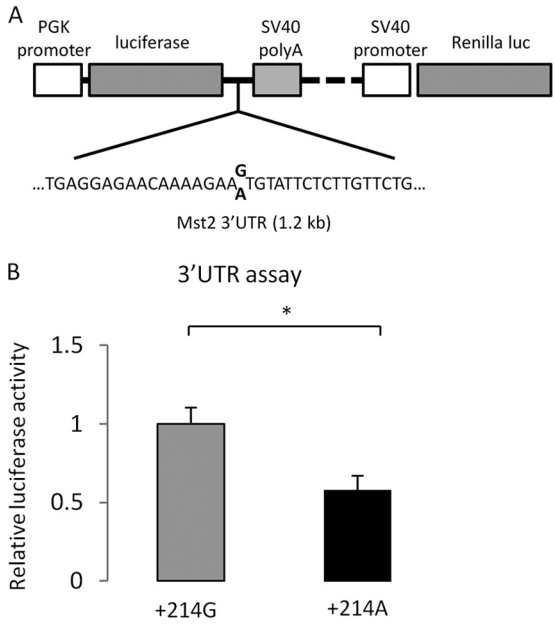

FIGURE 11. **Functional analysis of the human MST2 + 214G/A polymorphism.** *A*, schematic diagram of the luciferase constructs used for the experiment. The 1.2-kb 3′-UTR of the human *MST2* gene carrying either +214 G or A allele were inserted downstream of the luciferase-coding region. The expression of *Renilla* luciferase was used as a control for transfection efficiency. *B*, analysis using human primary fibroblasts indicated that the 3′-UTR bearing G allele produced significantly higher luciferase (*luc*) compared with 3′-UTR with A allele. (*, $p < 0.05$).

trols and suppresses the activation of YAP as we found that there was no difference in Mst1 expression between *Mst2*$^{-/-}$ mice and WT controls.

It is also important to note that in adult tissues, the response to Hippo pathway inhibition seems to be cell specific. Induction of proliferation occurred in cells of epithelial origin such as hepatocytes (6, 28) and intestinal epithelium (7). In contrast, in other cell types such as mouse embryonic fibroblasts, inactivation of Mst1 and Mst2 did not result in increased YAP activity (6). Our data adds to a growing body of evidence that in adult cardiomyocytes components of the Hippo pathway may regulate alternative pathways. For example, recent studies have demonstrated that Mst1 regulates apoptosis and autophagy in the heart (11–13). In addition, overexpression of Lats2, the downstream target of Mst1, resulted in the reduction of cardiomyocyte growth and protein synthesis as well as increased apoptosis (29).

Consistent with previous data, which showed that Mst1 positively induced cardiomyocyte apoptosis (11, 12), we found that ablation of Mst2 reduced cardiomyocyte apoptosis level following TAC. This process might be important with regard to the

difference in fibrosis level between WT and $Mst2^{-/-}$ mice after TAC. Although cardiac fibrosis levels were significantly less in $Mst2^{-/-}$ mice, we did not observe any difference in the cardiac fibroblast proliferation rate between knock-out and wild type. This suggests that the difference in fibrotic remodeling might be caused by an increased in reparative fibrosis due to the higher apoptosis level in WT mice.

Our mechanistic analyses suggest that Mst2 might regulate cardiomyocyte hypertrophic growth through modulation of Raf1 kinase, which subsequently activates prohypertrophic ERK1/2 kinases. The Raf1/ERK1/2 signaling cascade is involved in regulating cardiomyocyte growth as evidenced by observation in cultured cells as well as transgenic animals (24, 27, 30). It appears that the Mst2 kinase domain plays a key role in this process because the kinase inactive (K56R) mutant form of Mst2 failed to activate Raf1. However, it seems that inhibition of physical interaction between Mst2-Raf1 does not affect the activation of Raf1 and ERK1/2 by Mst2 because expression of mutant Mst2-ΔC, which does not interact with Raf1, is still able to induce ERK1/2 phosphorylation. However, analysis of phosphatase 2A catalytic C subunit (PP2A-C) expression indicates a possible involvement of this molecule in the regulation of Raf1 by Mst2, which is in agreement with previous published data by Kilili *et al.* (25). Indeed, further studies are still needed to precisely understand the regulatory mechanism of Raf1/ERK1/2 by Mst2. For example, it is not yet clear how Mst2 expression induces PP2A-C expression and why an intact kinase domain is needed in the modulation of Raf1/ERK1/2 activation.

Our data also point toward a potentially relevant role of an *MST2* polymorphism in human heart remodeling. Our initial study suggested a possible novel association between a polymorphism at the 3′-UTR of the human *MST2* gene (+214 G/A) with adverse remodeling in patients with mitral valve prolapse regardless of the regurgitant fraction. In addition, we show a molecular mechanism by which the polymorphism might be operative. Using a luciferase reporter system, we provide evidence that the polymorphism affects luciferase expression. Our data imply that individuals carrying a homozygous G allele may have higher Mst2 levels and hence exhibit more pronounced LV hypertrophy and remodeling, in agreement with our *in vivo* and *in vitro* models. However, these data should be regarded as preliminary, due to the relatively low number of patients used in this study, and thus, it should be tested in larger studies.

Overall, our results indicate that the Mst2-Raf1 signaling complex is a key regulator of pathological hypertrophy and remodeling in the heart. This complex mediates important downstream pathways in cardiomyocytes. Mst2 might therefore be a novel therapeutic target to reduce hypertrophy and adverse remodeling. Future studies need to be done to identify and develop novel inhibitor of this kinase and to test the effect on pathological hypertrophy.

REFERENCES

1. Hill, J. A., and Olson, E. N. (2008) Cardiac plasticity. *N. Engl. J. Med.* **358,** 1370–1380
2. Dorn, G. W., 2nd, Robbins, J., and Sugden, P. H. (2003) Phenotyping Hypertrophy, Eschew Obfuscation. *Circ. Res.* **92,** 1171–1175
3. Bergmann, O., Bhardwaj, R. D., Bernard, S., Zdunek, S., Barnabé-Heider, F., Walsh, S., Zupicich, J., Alkass, K., Buchholz, B. A., Druid, H., Jovinge, S., and Frisén, J. (2009) Evidence for cardiomyocyte renewal in humans. *Science* **324,** 98–102
4. Porrello, E. R., Mahmoud, A. I., Simpson, E., Hill, J. A., Richardson, J. A., Olson, E. N., and Sadek, H. A. (2011) Transient regenerative potential of the neonatal mouse heart. *Science* **331,** 1078–1080
5. Halder, G., and Johnson, R. L. (2011) Hippo signaling: growth control and beyond. *Development* **138,** 9–22
6. Zhou, D., Conrad, C., Xia, F., Park, J. S., Payer, B., Yin, Y., Lauwers, G. Y., Thasler, W., Lee, J. T., Avruch, J., and Bardeesy, N. (2009) Mst1 and Mst2 maintain hepatocyte quiescence and suppress hepatocellular carcinoma development through inactivation of the Yap1 oncogene. *Cancer Cell* **16,** 425–438
7. Zhou, D., Zhang, Y., Wu, H., Barry, E., Yin, Y., Lawrence, E., Dawson, D., Willis, J. E., Markowitz, S. D., Camargo, F. D., and Avruch, J. (2011) Mst1 and Mst2 protein kinases restrain intestinal stem cell proliferation and colonic tumorigenesis by inhibition of Yes-associated protein (Yap) overabundance. *Proc. Natl. Acad. Sci. U.S.A.* **108,** E1312–E1320
8. Heallen, T., Zhang, M., Wang, J., Bonilla-Claudio, M., Klysik, E., Johnson, R. L., and Martin, J. F. (2011) Hippo pathway inhibits Wnt signaling to restrain cardiomyocyte proliferation and heart size. *Science* **332,** 458–461
9. Xin, M., Kim, Y., Sutherland, L. B., Qi, X., McAnally, J., Schwartz, R. J., Richardson, J. A., Bassel-Duby, R., and Olson, E. N. (2011) Regulation of insulin-like growth factor signaling by Yap governs cardiomyocyte proliferation and embryonic heart size. *Sci. Signal* **4,** ra70
10. von Gise, A., Lin, Z., Schlegelmilch, K., Honor, L. B., Pan, G. M., Buck, J. N., Ma, Q., Ishiwata, T., Zhou, B., Camargo, F. D., and Pu, W. T. (2012) YAP1, the nuclear target of Hippo signaling, stimulates heart growth through cardiomyocyte proliferation but not hypertrophy. *Proc. Natl. Acad. Sci. U.S.A.* **109,** 2394–2399
11. Odashima, M., Usui, S., Takagi, H., Hong, C., Liu, J., Yokota, M., and Sadoshima, J. (2007) Inhibition of endogenous Mst1 prevents apoptosis and cardiac dysfunction without affecting cardiac hypertrophy after myocardial infarction. *Circ. Res.* **100,** 1344–1352
12. Yamamoto, S., Yang, G., Zablocki, D., Liu, J., Hong, C., Kim, S. J., Soler, S., Odashima, M., Thaisz, J., Yehia, G., Molina, C. A., Yatani, A., Vatner, D. E., Vatner, S. F., and Sadoshima, J. (2003) Activation of Mst1 causes dilated cardiomyopathy by stimulating apoptosis without compensatory ventricular myocyte hypertrophy. *J. Clin. Invest.* **111,** 1463–1474
13. Maejima, Y., Kyoi, S., Zhai, P., Liu, T., Li, H., Ivessa, A., Sciarretta, S., Del Re, D. P., Zablocki, D. K., Hsu, C. P., Lim, D. S., Isobe, M., and Sadoshima, J. (2013) Mst1 inhibits autophagy by promoting the interaction between Beclin1 and Bcl-2. *Nat. Med.* **19,** 1478–1488
14. Oh, S., Lee, D., Kim, T., Kim, T. S., Oh, H. J., Hwang, C. Y., Kong, Y. Y., Kwon, K. S., and Lim, D. S. (2009) Crucial Role for Mst1 and Mst2 Kinases in Early Embryonic Development of the Mouse. *Mol. Cell. Biol.* **29,** 6309–6320
15. Oceandy, D., Pickard, A., Prehar, S., Zi, M., Mohamed, T. M., Stanley, P. J., Baudoin-Stanley, F., Nadif, R., Tommasi, S., Pfeifer, G. P., Armesilla, A. L., Cartwright, E. J., and Neyses, L. (2009) Tumor suppressor Ras-association domain family 1 isoform A is a novel regulator of cardiac hypertrophy. *Circulation* **120,** 607–616
16. Oceandy, D., Cartwright, E. J., Emerson, M., Prehar, S., Baudoin, F. M., Zi, M., Alatwi, N., Venetucci, L., Schuh, K., Williams, J. C., Armesilla, A. L., and Neyses, L. (2007) Neuronal nitric oxide synthase signaling in the heart is regulated by the sarcolemmal calcium pump 4b. *Circulation* **115,** 483–492
17. Creasy, C. L., Ambrose, D. M., and Chernoff, J. (1996) The Ste20-like protein kinase, Mst1, dimerizes and contains an inhibitory domain. *J. Biol. Chem.* **271,** 21049–21053
18. Armesilla, A. L., Williams, J. C., Buch, M. H., Pickard, A., Emerson, M., Cartwright, E. J., Oceandy, D., Vos, M. D., Gillies, S., Clark, G. J., and Neyses, L. (2004) Novel functional interaction between the plasma membrane Ca2+ pump 4b and the proapoptotic tumor suppressor Ras-associated factor 1 (RASSF1). *J. Biol. Chem.* **279,** 31318–31328
19. Schiller, N. B., Shah, P. M., Crawford, M., DeMaria, A., Devereux, R., Feigenbaum, H., Gutgesell, H., Reichek, N., Sahn, D., and Schnittger, I. (1989) Recommendations for quantitation of the left ventricle by two-dimensional echocardiography. American Society of Echocardiography

Committee on Standards, Subcommittee on Quantitation of Two-Dimensional Echocardiograms. *J. Am. Soc. Echocardiogr.* **2,** 358–367
20. Rokey, R., Sterling, L. L., Zoghbi, W. A., Sartori, M. P., Limacher, M. C., Kuo, L. C., and Quinones, M. A. (1986) Determination of regurgitant fraction in isolated mitral or aortic regurgitation by pulsed Doppler two-dimensional echocardiography. *J. Am. Coll. Cardiol.* **7,** 1273–1278
21. Devereux, R. B., Alonso, D. R., Lutas, E. M., Gottlieb, G. J., Campo, E., Sachs, I., and Reichek, N. (1986) Echocardiographic assessment of left ventricular hypertrophy: comparison to necropsy findings. *Am. J. Cardiol.* **57,** 450–458
22. Romano, D., Matallanas, D., Weitsman, G., Preisinger, C., Ng, T., and Kolch, W. (2010) Proapoptotic kinase MST2 coordinates signaling crosstalk between RASSF1A, Raf-1, and Akt. *Cancer Res.* **70,** 1195–1203
23. O'Neill, E., Rushworth, L., Baccarini, M., and Kolch, W. (2004) Role of the kinase MST2 in suppression of apoptosis by the proto-oncogene product Raf-1. *Science* **306,** 2267–2270
24. Harris, I. S., Zhang, S., Treskov, I., Kovacs, A., Weinheimer, C., and Muslin, A. J. (2004) Raf-1 kinase is required for cardiac hypertrophy and cardiomyocyte survival in response to pressure overload. *Circulation* **110,** 718–723
25. Kilili, G. K., and Kyriakis, J. M. (2010) Mammalian Ste20-like kinase (Mst2) indirectly supports Raf-1/ERK pathway activity via maintenance of protein phosphatase-2A catalytic subunit levels and consequent suppression of inhibitory Raf-1 phosphorylation. *J. Biol. Chem.* **285,** 15076–15087
26. Ohori, M., Kinoshita, T., Okubo, M., Sato, K., Yamazaki, A., Arakawa, H., Nishimura, S., Inamura, N., Nakajima, H., Neya, M., Miyake, H., and Fujii, T. (2005) Identification of a selective ERK inhibitor and structural determination of the inhibitor-ERK2 complex. *Biochem. Biophys. Res. Commun.* **336,** 357–363
27. Bueno, O. F., De Windt, L. J., Tymitz, K. M., Witt, S. A., Kimball, T. R., Klevitsky, R., Hewett, T. E., Jones, S. P., Lefer, D. J., Peng, C. F., Kitsis, R. N., and Molkentin, J. D. (2000) The MEK1-ERK1/2 signaling pathway promotes compensated cardiac hypertrophy in transgenic mice. *EMBO J.* **19,** 6341–6350
28. Song, H., Mak, K. K., Topol, L., Yun, K., Hu, J., Garrett, L., Chen, Y., Park, O., Chang, J., Simpson, R. M., Wang, C. Y., Gao, B., Jiang, J., and Yang, Y. (2010) Mammalian Mst1 and Mst2 kinases play essential roles in organ size control and tumor suppression. *Proc. Natl. Acad. Sci. U.S.A.* **107,** 1431–1436
29. Matsui, Y., Nakano, N., Shao, D., Gao, S., Luo, W., Hong, C., Zhai, P., Holle, E., Yu, X., Yabuta, N., Tao, W., Wagner, T., Nojima, H., and Sadoshima, J. (2008) Lats2 is a negative regulator of myocyte size in the heart. *Circ. Res.* **103,** 1309–1318
30. Glennon, P. E., Kaddoura, S., Sale, E. M., Sale, G. J., Fuller, S. J., and Sugden, P. H. (1996) Depletion of mitogen-activated protein kinase using an antisense oligodeoxynucleotide approach downregulates the phenylephrine-induced hypertrophic response in rat cardiac myocytes. *Circ. Res.* **78,** 954–961

The Mammalian Ste20-like Kinase 2 (Mst2) Modulates Stress-induced Cardiac Hypertrophy

Min Zi, Arfa Maqsood, Sukhpal Prehar, Tamer M. A. Mohamed, Riham Abou-Leisa, Abigail Robertson, Elizabeth J. Cartwright, Simon G. Ray, Sangphil Oh, Dae-Sik Lim, Ludwig Neyses and Delvac Oceandy

J. Biol. Chem. 2014, 289:24275-24288.
doi: 10.1074/jbc.M114.562405 originally published online July 17, 2014
